

monkey: The reaction time in an arm-reaching paradigm could be predicted from the ongoing activity preceding the arm movement (20).

REFERENCES AND NOTES

1. P. H. Schiller, B. L. Finlay, S. F. Volman, *Brain Res.* **105**, 347 (1976); P. Heggelund and K. Albus, *Exp. Brain Res.* **32**, 197 (1978); R. P. Scobey and A. J. Gabor, *ibid.* **77**, 398 (1989).
2. R. Vogels, W. Spileers, G. A. Orban, *Exp. Brain Res.* **77**, 432 (1989); R. J. Snowden, S. Treue, R. A. Andersen, *ibid.* **88**, 389 (1992); W. R. Softky and C. Koch, *J. Neurosci.* **13**, 334 (1993).
3. W. A. Rosenblith, Ed., *Processing Neuroelectric Data* (MIT Press, Cambridge, MA, 1959); G. L. Gerstein, *Science* **131**, 1811 (1960).
4. E. R. John, *Science* **177**, 850 (1972); G. L. Shaw, E. Harth, A. B. Scheibel, *Exp. Neurol.* **77**, 324 (1982); K. H. Britten, M. N. Shadlen, W. T. Newsome, W. A. Movshon, *J. Neurosci.* **12**, 4745 (1992).
5. Z. F. Mainen and T. J. Sejnowski, *Science* **268**, 1503 (1995).
6. E. Hartveit and P. Heggelund, *J. Neurophysiol.* **72**, 1278 (1994); F. Mechler, R. Shapley, M. J. Hawken, *Soc. Neurosci. Abstr.* **21**, 22 (1995); G. R. Holt, W. R. Softky, C. Koch, R. J. Douglas, *ibid.*, p. 22; W. S. Geisler and D. G. Albrecht, *Vision Res.* **35**, 2723 (1995); H. E. Wheat, A. W. Goodwin, A. S. Browning, *J. Neurosci.* **15**, 5582 (1995); M. N. Shadlen, K. H. Britten, W. T. Newsome, J. A. Movshon, *ibid.* **16**, 1486 (1996).
7. M. N. Shadlen and W. T. Newsome, *Curr. Opin. Neurobiol.* **4**, 569 (1994); D. Ferster and N. Spruston, *Science* **270**, 756 (1995).
8. A. Arieli, D. Shoham, R. Hildesheim, A. Grinvald, *J. Neurophysiol.* **73**, 2072 (1995).
9. Preliminary results were presented in abstract form [A. Arieli, A. Sterkin, A. Grinvald, A. Aertsen, *Soc. Neurosci. Abstr.* **21**, 772 (1995)].
10. Surgery was performed under aseptic conditions and deep anesthesia. All procedures were carried out in accordance with the National Institutes of Health and Weizmann Institute regulations for animal care.
11. A. Grinvald, A. Manker, M. Segal, *J. Physiol.* **333**, 269 (1982); A. Grinvald, L. Anglister, J. A. Freeman, R. Hildesheim, A. Manker, *Nature* **308**, 848 (1984); H. S. Orbach, L. B. Cohen, A. Grinvald, *J. Neurosci.* **5**, 1886 (1985); A. Grinvald, R. D. Frostig, E. Lieke, R. Hildesheim, *Physiol. Rev.* **68**, 1285 (1988).
12. A. Grinvald, E. E. Lieke, R. D. Frostig, R. Hildesheim, *J. Neurosci.* **14**, 2545 (1994).
13. Components not related to the neuronal activity were removed from the optical signals. Those components originate from changes in light absorption by hemoglobin with every heartbeat or from movement of the cortical tissue as a result of heart pulsation and respiration. Using the fact that the heartbeat artifact is synchronized with the electrocardiogram (ECG), we eliminated the artifact by subtracting the ECG-triggered average optical signal from the raw data at each heartbeat (8, 14). This "cleaning" procedure was recently improved by analogous elimination of the respiratory wave. The two series of images that were thus removed from the data are referred to as the artifact. Before application of this cleaning procedure, the average correlation coefficient between the optical images and the artifact was 0.8; after this procedure, the correlation dropped to 0.02 (A. Sterkin *et al.*, in preparation).
14. G. Gratton and P. M. Corballis, *Psychophysiology* **32**, 292 (1995).
15. R. Cooper, A. L. Winter, H. J. Crow, W. G. Walter, *Electroencephalogr. Clin. Neurophysiol.* **18**, 217 (1965); R. Elul, *Int. Rev. Neurobiol.* **15**, 227 (1972); O. D. Creutzfeldt and J. Houchin, in *Electrical Activity from the Neuron to the EEG and EMG*, vol. 2C of *Handbook of Electroencephalography and Clinical Neurophysiology*, O. D. Creutzfeldt, Ed. (Elsevier, Amsterdam, 1974), pp. 5-54.
16. A. S. Gevins and R. E. Schaffer, *Crit. Rev. Bioeng.* **1**, 113 (1980); D. Regan, *Human Brain Electrophysiol-*

ogy: Evoked Potentials and Evoked Magnetic Fields in Science and Medicine (Elsevier, New York, 1989).

17. M. Abeles, H. Bergman, E. Margalit, E. Vaadia, *J. Neurophysiol.* **70**, 1629 (1993); W. Blair, C. Koch, W. T. Newsome, K. H. Britten, *Soc. Neurosci. Abstr.* **20**, 1279 (1994).
18. Part of the linearity is presumably caused by the fact that these measurements reflect synaptic population activity. Therefore, they are subject to a linearizing effect similar to that reported previously for evoked potentials [H. Spekreijse and L. H. van der Tweel, *Nature* **205**, 913 (1965)]. For single-neuron activity we would expect a more prominent nonlinear behavior (for example, related to the firing threshold). The observed reduction in correlation between ongoing activity and single-neuron firing rate (Fig. 2D) is con-

sistent with this.

19. A. Arieli, in *Information Processing in the Cortex: Experiments and Theory*, A. Aertsen and V. Braitenberg, Eds. (Springer-Verlag, Berlin, 1992), pp. 123-138.
20. _____ *et al.*, *Soc. Neurosci. Abstr.*, in press.
21. We thank E. Ahissar, Y. Fregnac, R. Malach, D. Sagi, W. von Seelen, M. Segal, D. Shoham, I. Steinberg, S. Ullman, and E. Vaadia for their constructive comments. Supported in part by grants from the Wolfson Foundation; the Israel Science Foundation, administered by the Israel Academy of Sciences and Humanities; the Minerva Foundation, Munich, Germany; and from the Human Frontier Science Program.

19 March 1996; accepted 16 July 1996

Temporal Hierarchical Control of Singing in Birds

Albert C. Yu and Daniel Margoliash*

Songs of birds comprise hierarchical sets of vocal gestures. In zebra finches, songs include notes and syllables (groups of notes) delivered in fixed sequences. During singing, premotor neurons in the forebrain nucleus HVC exhibited reliable changes in activity rates whose patterns were uniquely associated with syllable identity. Neurons in the forebrain nucleus robustus archistriatalis, which receives input from the HVC, exhibited precisely timed and structured bursts of activity that were uniquely associated with note identity. Hence, units of vocal behavior are represented hierarchically in the avian forebrain. The representation of temporal sequences at each level of the hierarchy may be established by means of a decoding process involving interactions of higher level input with intrinsic local circuitry. Behavior is apparently represented by precise temporal patterning of spike trains at lower levels of the hierarchy.

The neural codes that define discrete units of episodic behavior and organize these units into temporal sequences are not well established. Vocalizations constitute a group of behaviors for which correct temporal sequencing of discrete, often stereotyped events is fundamental to proper execution (1). Participation of midbrain structures in the generation of simple calls is well known in both mammals and birds (2). Less is known about the contribution of forebrain structures, particularly in the production of more complex vocalizations such as human speech and bird songs. Here, we characterize singing-related neuronal activity in the nuclei HVC and robustus archistriatalis (RA) of the zebra finch (*Taeniopygia guttata*). We present evidence for the hierarchical organization of neural codes that corresponds to the hierarchical organization of the singing behavior.

Zebra finch songs are hierarchically organized vocalizations formed by discrete acoustic elements (syllables) separated by

intervals of silence (3). Song syllables can be classified into distinct classes (types) on the basis of acoustic features. Each syllable, in turn, can be further divided into acoustically distinct notes. The typical zebra finch song begins with a variable number of identical, simple introductory syllables comprising one or two notes, followed by a fixed sequence (motif) of multinote syllables. The motifs are repeated in longer versions of songs and are often separated by introductory syllables or other simple "connecting" syllables.

We developed techniques to record single-unit and multiple-unit neuronal activity in the HVC and RA of singing adult male zebra finches (4). Multiple sites were recorded in each nucleus in several birds who were good singers, resulting in a large database of vocalizations and associated neuronal activities [94 ± 92 (mean ± SD) songs per bird, n = 13 birds]. The onset and offset time and the identity of each syllable and note were established manually or by an automatic technique (5) whose output was verified manually. This procedure was essential for veridical analysis because the exact timing of the sequence of song elements varied from song to song. Additional long records (300 s) of ongoing activity

A. C. Yu, Committee on Neurobiology, University of Chicago, Chicago, IL 60637, USA.

D. Margoliash, Department of Organismal Biology and Anatomy, University of Chicago, Chicago, IL 60637, USA.

*To whom correspondence should be addressed.

during behavioral quiescence were collected to quantify baseline activity.

Each HVC unit was strongly recruited starting before the first introductory syllable, with overall excitation throughout the entire duration of the song and with activity terminating before the end of the song (Fig. 1, A and B). We determined the exact pattern of activation by calculating motor activity histograms (MAHs), representing

each unit's activity relative to the onset of a syllable or note type (6). For each HVC neuron, activity levels close to the maximum firing rate were found during the production of almost all syllable types. Each syllable type was associated with a stable and unique pattern of neuronal activity (Fig. 1B). The activity pattern for the same syllable type varied across HVC neurons, and for each HVC neuron, the activity pat-

tern varied with syllable type. Temporal features of neuronal activity associated with each syllable type were sufficiently distinctive that correct inference of vocal output could be easily made in many instances by inspection of the associated MAH. Aligning neuronal activity with the onset (or offset) of the associated syllable was essential for detecting these features. The distinct features of the MAHs were lost when the onset or offset of one syllable was used

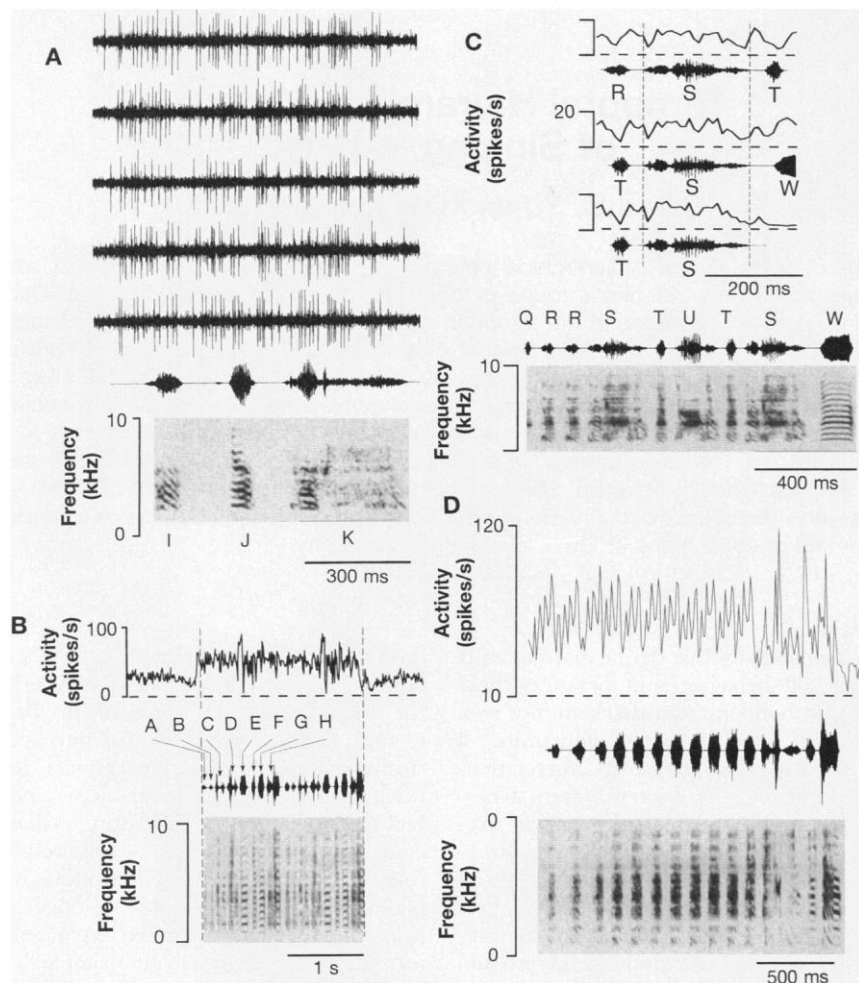


Fig. 1. (A) Activity patterns of HVC neuron ZF_WT25_18 during production of a song motif formed by a sequence of three syllables (I-J-K). The five neuronal traces (top traces) show the loose organization of bursts of activity preceding each syllable. Neuronal traces were aligned at the onset of syllable K (the exact timing of syllable onsets and offsets was slightly different for each neuronal trace). The oscillograph (amplitude envelope) and spectrograph (frequency representation) of an exemplar of the motif are time-aligned below the neuronal traces, and the syllable type designation is indicated below the spectrograph. **(B)** HVC activity during a song with two motifs. An extended MAH (eMAH; top trace) (20) of neuron ZF_YL49_4 shows the similarity of HVC activity across two song motifs (note similar peaks of activity around syllable E). The oscillograph and spectrograph of the canonical song of the bird are shown in the middle and bottom traces, respectively, and the syllable type designation is indicated above the oscillograph. Vertical dashed lines indicate the relative positions of song onset and offset. **(C)** Activity of HVC neuron ZF_GR46_2 for syllable S in different contexts (syllable sequences). The top three traces show eMAHs corresponding to three different sequences in which syllable S occurs (R-S-T, $n = 137$ entries; T-S-W, $n = 133$ entries; T-S-end of song, $n = 67$ entries). Vertical dashed lines indicate onset and offset of syllable S. The oscillograph and spectrograph of the canonical song are shown in the middle and bottom traces, respectively. **(D)** Similarity of HVC activity for the repeated syllables in introductory sequences of songs. An eMAH of neuron ZF_GR43_1 (top trace) is time aligned with the oscillograph and spectrograph (bottom traces) of the canonical song. The typical song of ZF_GR43 was unusual, with many introductory syllables but only one motif.

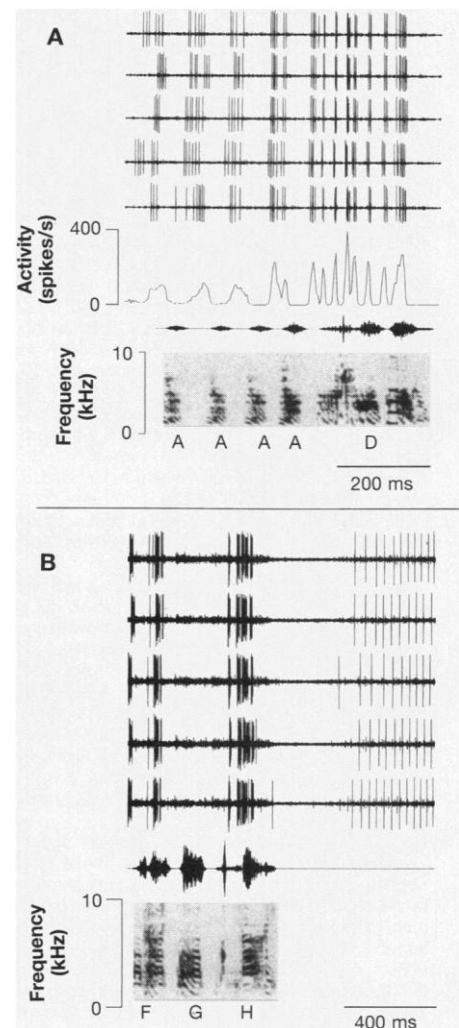


Fig. 2. (A) Activity patterns of RA neuron ZF_RA01_7 during a sequence of introductory syllables followed by the first syllable of the motif. Neuronal traces were aligned at the onset of syllable D. Individual MAHs that contributed to the eMAH were calculated starting 40 ms before their corresponding syllable. **(B)** Activity patterns of RA neuron ZF_RA02_5 during a motif that ends a song. Neuronal traces were aligned at the onset of syllable H. There was strong inhibition, lasting 400 to 800 ms, after song offset in all RA neurons, after which the neurons returned to their nonsinging ongoing oscillatory activity. In contrast, excitation is seen in the background during suppression of activity associated with syllable G. Other single units recorded in bird ZF_RA02 exhibited excitation during syllable G.

to calculate the MAH for even immediately preceding or following syllables. This effect resulted primarily from variation across songs in the intervals between syllables (there was much lower variation in the duration of syllables), demonstrating that the strong modulation of neuronal activity in HVC during singing was related to the timing of syllables.

In all birds, MAHs for syllables of the same type occurring in different motifs of a song were strikingly similar (Fig. 1B). To quantify this, we calculated the linear correlation coefficient r for pairs of MAHs corresponding to syllables of the same type and for pairs of MAHs corresponding to syllables of different types (7). Correlations were high comparing pairs of MAHs from the same neuron for syllables of the same type drawn from different motifs ($r = 0.918 \pm 0.05$, $n = 644$ MAH pairs). By comparison, correlations were very low between pairs of MAHs from the same neuron for different syllable types drawn from the first motifs ($r = 0.042 \pm 0.263$, $n = 497$ MAH pairs). The two distributions of correlation coefficients were nonoverlapping (Mann-Whitney U test, $Z = -28.997$, $P = 0.0001$). Additionally, several birds produced songs in which syllables of a given

type occurred in two or more distinct sequences (different preceding or following syllables, or where the focal syllable ended the song) (Fig. 1C). Without fail, syllables of the same type occurring in different syllable sequences also had similar MAHs ($r = 0.919 \pm 0.065$, $n = 14$ MAH pairs, four birds). The repeated introductory syllables at the beginning of a song also presented the same MAHs whether in the middle of a sequence of such syllables or as the last syllable before the first motif ($r = 0.895 \pm 0.112$, $n = 78$ MAH pairs, nine birds) (Fig. 1D). These observations demonstrate that motor activity in the zebra finch HVC is centered on the syllable, is based on syllable type, and is independent of syllable context.

In contrast to the relatively tonic discharge patterns of HVC neurons, neuronal activity in the RA during singing was characterized by trains of short bursts of spikes separated by periods of profound inhibition (Fig. 2, A and B). The spike bursts associated with all introductory syllables up to the last one had imprecise and variable timing (compare Figs. 1D and 2A). Otherwise, each spike burst was characterized by a stereotyped and unique pattern of intraburst timing. The reliability of activity patterns was sufficient to allow correct inference of

vocal output from individual spike trains. The RA neurons could be recruited after the onset of some syllable types, remain active after the offset of some syllable types, or exhibit complete suppression of activity even for complex syllables that formed part of a motif (Fig. 2B), phenomena never observed for HVC neurons.

During singing, each RA spike burst pattern was associated with a unique subsyllabic acoustic event. For example, two of the four birds sang a pair of syllable types that had different initial note types but thereafter shared the same sequence of note types (Fig. 3). For these four syllable types, all of the RA neurons ($n = 8$) exhibited similar activity patterns corresponding to the shared note types ($r = 0.883 \pm 0.081$,

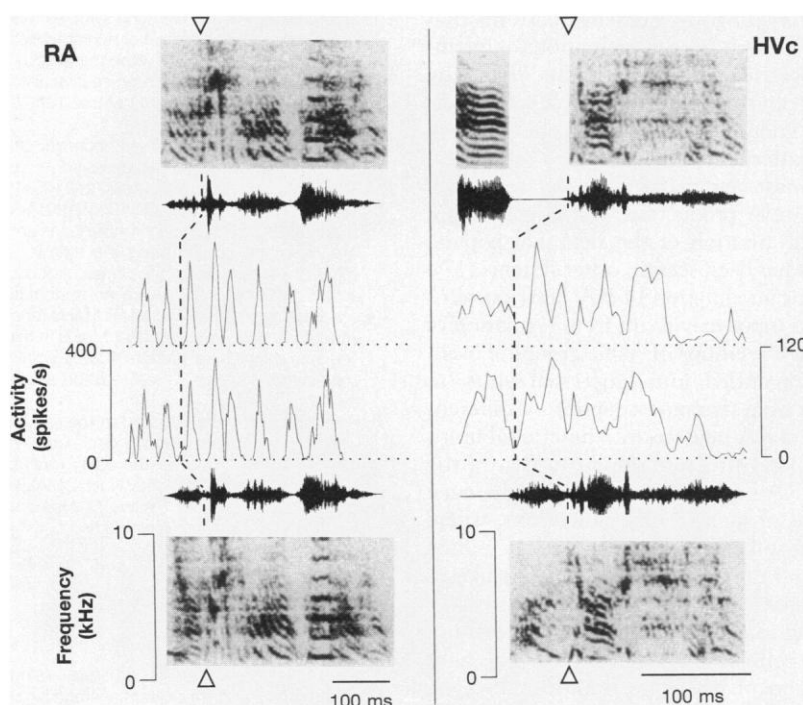


Fig. 3. MAHs for syllable pairs that start with different note types but otherwise comprise the same sequence of notes. (**Left**) Two syllables of bird ZF_RA01 share the same sequence of notes, except for different introductory notes (to the left of the open triangles). MAHs are shown for RA neuron ZF_RA01_7 for the two syllable types (top MAH, $n = 91$ entries; bottom MAH, $n = 85$). The dashed line through the MAHs marks 40 ms before the start of the first shared note. (**Right**) An equivalent analysis for HVC neuron ZF_WT25_18 for two similar syllable types. One syllable type (bottom panel, associated MAH has 70 entries) has an introductory note that is missing from the other syllable type (top panel, associated MAH has 93 entries).

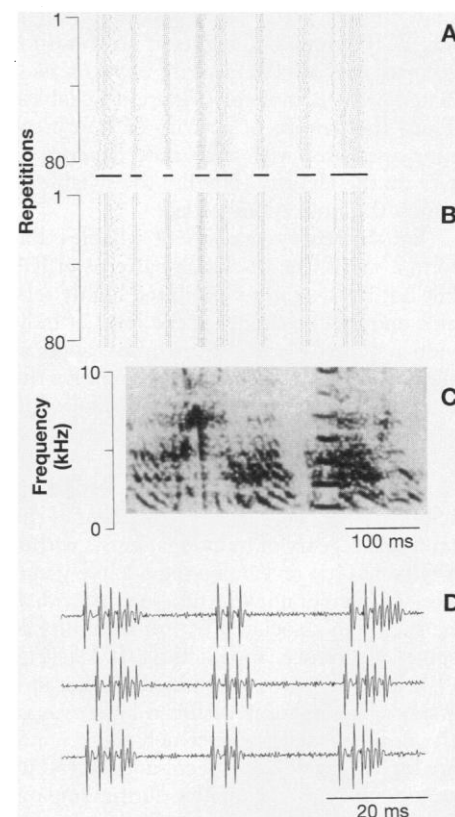


Fig. 4. (**A** and **B**) The discharge pattern of an RA neuron during 86 occurrences of the same syllable type. In (**A**), the time of each spike train is adjusted relative to the acoustics of the corresponding syllables by a cross-correlation technique (9). In (**B**), the same spike data are aligned on a per-burst basis, minimizing time differences (10). The horizontal bars below (**A**) indicate the time windows used to define each burst. (**C**) The spectrogram of the syllable, time-aligned with (**A**) and (**B**). (**D**) The burst pattern of another RA neuron, demonstrating reduction in spike amplitude for very fast bursts. As in this case, we commonly observed that the first interspike intervals of very fast bursts were of longer duration than the subsequent interspike intervals, which were relatively constant in duration.

$n = 8$ comparisons of MAHs corresponding to the sequence of notes of the same type) and dissimilar activity patterns corresponding to the dissimilar note types drawn from the same syllables ($r = 0.190 \pm 0.304$, $n = 8$ comparisons of MAHs) (8). Thus, the pattern of activity of RA neurons depends on note type. There were also two examples of birds with HVC recordings who sang a pair of syllable types that differed in the sequence of initial note types but shared the same sequence of subsequent note types. In contrast to the RA neurons, however, all HVC neurons ($n = 12$) displayed dissimilar MAHs for all segments of these similar syllable types (Fig. 3). For HVC neurons, the correlation coefficients for MAHs corresponding to the sequence of notes of the same type were low ($r = 0.401 \pm 0.158$, $n = 12$ comparisons of MAHs), much lower than those for the corresponding analysis for RA neurons but higher than those for comparisons of HVC activity patterns associated with completely different syllables. Thus, the pattern of activity of HVC neurons associated with each note depends in part on the identity (type) of the syllable in which the note is embedded.

For the fixed sequences of syllables that form a motif, the discharge patterns of RA but not HVC neurons exhibited highly reliable and precise timing at the level of individual spikes. For all RA neurons, application of an analysis procedure to improve the temporal registry of syllables (9) resulted in a visually striking alignment of bursts, exposing a consistent temporal structure within each burst, albeit with some remaining temporal jitter (Fig. 4A). Adjustment of the temporal registry of individual bursts within a syllable (10) revealed a remarkable precision of temporal patterning in individual bursts, often associated with a reliability of spike occurrence approaching 100% (Fig. 4B). In many cases, the temporal jitter at a given spike position within a burst was of the order of the rate at which the original analog wave forms had been sampled ($50 \mu\text{s}$ per sample). Additionally, during singing, RA neurons operated through most of the dynamic range of activity available to nervous systems. Against a background of complete suppression of activity, some neurons exhibited zero or one spike for a given syllable, whereas the spike rate of the fastest burst for each neuron was 383 ± 119 spikes/s ($n = 15$ neurons), in many cases with consistent intraburst instantaneous spike rates > 700 Hz. For many neurons, we observed bursts that consistently drove the neuron into its relative refractory period, causing dramatic reduction in spike amplitude and potentially approaching spike failure (Fig. 4D). Thus, the stereotype of bird song is achieved by means of a neuronal

code within the forebrain (RA) operating over a wide dynamic range that exhibits precise and reliable temporal patterning of spikes.

Singing is a motor program, representing the coordinated spatiotemporal activation of many syringeal and vocal tract muscles in conjunction with the respiratory and postural systems (11). Our data indicate that in the zebra finch, successively smaller units of vocalization—syllables and presumptively notes—are reliably coded in the activity patterns of single HVC and RA neurons, respectively [compare with (12)]. The physiological signature of a note depends on note sequence in HVC and is independent of note sequence in RA. Thus, on the basis of these data, the precise sequencing of notes apparently emerges from the interaction of HVC input with RA local circuits. Similarly, the temporal sequence of syllables may result from an interaction of afferent input to HVC (13) with local HVC circuitry. These data imply a hierarchical organization for the forebrain control of bird song production (14). A hierarchical organization has long been anticipated in the neural control of behavior (15).

Our results indicate that the neural code for syllables (movements) is transformed in the projection of HVC onto RA (motor control). Neurons of the RA have simple, oscillatory, ongoing discharge patterns that probably result from combinations of intrinsic properties and local circuits (16). The driving and coupling of simple oscillators could produce during singing the complex burst patterns that we observed. Such processes must be dynamically regulated at the rate of note production, resulting in rapid resynchronization of the neuronal population, as has been seen in other systems (17). Dynamic modulation of RA burst patterns by HVC input may result from regulation of the phase relations of stable groups of oscillators organized into functional units, as well as from dynamic coupling of different groups of RA neurons into functional units. A temporal structure similar to that of the fastest RA bursts has been seen in the burst patterns of inferior olivary neurons, where the first spike results from a somatic sodium spike and the timing of subsequent spikes is modulated by dendritic calcium influx (18). Bursting in the RA is under the control of similar cellular mechanisms (16). The tight regulation of discharge timing in the RA suggests that information is coded in the temporal structure of the bursts. Temporal patterns of neural activity may convey information in other systems as well (19). An analysis of such patterning in relation to the behavioral requirements of the animal can lead to explication of the nature and function of the putative temporal codes.

1. K. S. Lashley, in *Cerebral Mechanisms in Behavior*, L. A. Jeffress, Ed. (Wiley, New York, 1951), pp. 112–135; M. Konishi, in *Perception*, vol. VIII of *Handbook of Sensory Physiology*, R. Held, H. W. Leibowitz, H.-L. Teuber, Eds. (Springer-Verlag, Berlin, 1978), pp. 289–309; P. Marler and S. Peters, *Science* **198**, 519 (1977); P. Marler and R. Pickert, *Anim. Behav.* **32**, 673 (1984); H. C. Gerhardt, *J. Exp. Biol.* **74**, 59 (1978); R. R. Hoy and R. C. Paul, *Science* **180**, 82 (1973).
2. D. Ploog, *Brain Res. Rev.* **3**, 35 (1981); T. J. Seller, *Trends Neurosci.* **4**, 301 (1981).
3. K. Immelmann, in *Bird Vocalizations*, R. A. Hinde, Ed. (Cambridge Univ. Press, London, 1969), pp. 61–74; R. A. Zann, *The Zebra Finch* (Oxford Univ. Press, Oxford, 1996).
4. All procedures were approved by an institutional animal care committee. Under pentobarbital and chloral hydrate anesthesia, male zebra finches were implanted with headgear, including electrodes and electronics. After recovery, a bird typically participated in 6- to 8-hour recording sessions every 2 to 3 days. We achieved stable chronic recordings in HVC by using bundles of Isonel-insulated microwires (eight recording sites, seven birds) or a custom-built 1-g mechanical microdrive to simultaneously move four Pt-Ir electrodes (15 HVC recording sites in two birds, and 22 RA recording sites in four birds). There were no systematic differences noted in the activity patterns of HVC neurons recorded under the two conditions, and the data were combined in all analyses presented here. During a recording session, the bird was attached to a custom-built commutator by a flexible cable, permitting free exploration inside the cage. In some cases we collected data while zebra finches sang spontaneously; otherwise, females or mirrors were introduced into the adjacent half-cages to stimulate directed song [R. Sossinka and J. Böhner, *Z. Tierpsychol.* **53**, 123 (1980)]. During data analysis, female calls could be distinguished from male calls and from male song syllables. After a bird was killed with an overdose of pentobarbital, the position of the recording sites within the target nuclei was confirmed with standard frozen-section histology.
5. S. E. Anderson, A. S. Dave, D. Margoliash, *J. Acoust. Soc. Am.* **100**, 1209 (1996).
6. Single units were isolated (categorized) off-line according to established procedures [M. L. Sutter and D. Margoliash, *J. Neurophysiol.* **72**, 2105 (1994); M. S. Lewicki, *Neural Comp.* **6**, 1005 (1994)]. We constructed MAHs by aligning vocalizations and the related neuronal activity using the syllable onset or offset times, then binning the times of occurrence of action potentials. There were no systematic differences between onset and offset MAHs for either the HVC or RA data; we use onset MAHs in this report. The data shown here are from 40 well-isolated single units in the HVC and 23 well-isolated single units in the RA.
7. Pairs of MAHs were adjusted to the same duration with the use of time-warping decimation-interpolation techniques implemented using routines in the Matlab program (MathWorks, Natick, MA). The linear correlation coefficient r for two MAHs representing syllables x and y was calculated as

$$r = \frac{\sum_i (x_i - \bar{x})(y_i - \bar{y})}{\sqrt{\sum_i (x_i - \bar{x})^2} \sqrt{\sum_i (y_i - \bar{y})^2}} \quad (1)$$

where x_i and y_i represent individual histogram bin values, and \bar{x} and \bar{y} represent average bin values.

8. The MAHs were separated into two segments: one segment associated with shared note types, and one segment associated with dissimilar note types. The segmentation assumed that neuronal activity preceded the vocalizations by 40 ms for the RA recordings and by 50 ms for the HVC recordings. These values correspond to average multiunit latency preceding singing [J. S. McCasland and M. Konishi, *Proc. Natl. Acad. Sci. U.S.A.* **78**, 7815 (1981)].
9. Spike trains were brought into temporal registry by

cross-correlating the corresponding syllables, as follows. Introductory syllables were excluded because for the RA they are not associated with a precise temporal pattern of activity (Fig. 2A). Motif syllables comprising simple harmonic stacks were also excluded because they lack meaningful time-varying frequency modulation, which resulted in unreliable cross-correlations. This left acoustically complex syllables of motifs for analysis. The acoustic records were scored without reference to the associated spike trains to eliminate recordings with acoustic clutter (background cage noises, calls of females). Six additional syllables were eliminated on this basis because less than 10 acoustically uncontaminated exemplars were identified, preventing meaningful statistical analysis. For each of the 15 resultant syllable types (15 neurons, three birds), a "referent" syllable was chosen by manual inspection of spectrographs of the set of exemplar syllables. The spectrograph of each exemplar syllable was then cross-correlated with the spectrograph of the referent [C. W. Clark, P. Marler, P. Beeman, *Ethology* **76**, 101 (1987)]. We then adjusted the temporal registry of each spike train associated with each exemplar syllable, relative to the spike train associated with the referent syllable, by applying a shift in time (translation) based on the position of the peak in the correlation function. The time shifts were typically quite small ($\tau = 3.00 \pm 2.31$ ms, $n = 1436$ cross-correlations of referent and exemplar syllables), implying that the original manual segmentation was quite accurate; nevertheless, this shift significantly affected the temporal registry of spike trains.

10. An optimal translation of the spike trains was applied on a burst-by-burst basis to minimize the global difference in spike timing. That is, this procedure aligned each spike burst independent of the acoustics of associated notes. The acoustic procedure of (9) failed to further improve the temporal registry of spike bursts when applied on a note-by-note basis. This failure may be the result of the fine temporal resolution of RA neuronal discharge patterns overwhelming inherent limitations in time-frequency resolution in the calculation of spectrographs based on short-time Fourier transformations [G. D. Bergland, *IEEE Spectrum* **7**, 41 (1969)]. Nevertheless, it implies that we were not able to quantitatively demonstrate that the timing of each burst pattern was associated with the timing of each note. The RA exhibits a myotopic organization [D. S. Vicario, *J. Neurobiol.* **22**, 63 (1991)], hence the activity of RA neurons may be associated with activation of individual muscles or groups of muscles.
11. S. Nowicki and R. R. Capranica, *Science* **231**, 1297 (1986); F. Goller and R. A. Suthers, *Nature* **373**, 63 (1995); M. W. Westneat, J. H. J. Long, W. Hoese, S. Nowicki, *J. Exp. Biol.* **182**, 147 (1993).
12. E. E. Fetz, in *Movement Control*, P. Cordo and S. Harnad, Eds. (Cambridge Univ. Press, Cambridge, 1994), pp. 77–88.
13. H. Williams and D. Vicario, *J. Neurobiol.* **24**, 903 (1993).
14. See also E. T. Vu, M. E. Mazurek, Y.-C. Kuo, *J. Neurosci.* **14**, 6924 (1994).
15. N. Tinbergen, *Symp. Soc. Exp. Biol.* **4**, 305 (1950); *The Study of Instinct* (Oxford Univ. Press, Oxford, 1951).
16. R. Mooney, *J. Neurosci.* **12**, 2464 (1992).
17. M. Abeles et al., *Proc. Natl. Acad. Sci. U.S.A.* **92**, 8616 (1995); E. Vaadia et al., *Nature* **373**, 515 (1995).
18. R. Llinás, *Cold Spring Harbor Symp. Quant. Biol.* **55**, 933 (1990).
19. C. E. Carr, W. Heiligenberg, G. J. Rose, *J. Neurosci.* **6**, 107 (1986); C. E. Carr and M. Konishi, *Proc. Natl. Acad. Sci. U.S.A.* **85**, 8311 (1988); E. Ahissar et al., *Science* **257**, 1412 (1992); G. H. Recanzone, M. M. Merzenich, C. E. Schreiner, *J. Neurophysiol.* **67**, 1071 (1992); J. C. Middlebrooks, A. E. Clock, L. Xu, D. M. Green, *Science* **264**, 842 (1994); R. C. de Charms and M. M. Merzenich, *Nature* **381**, 610 (1996); W. Bair and C. Koch, *Neural Comp.* **8**, 1184 (1996).
20. To construct an eMAH, we defined a canonical song: the most common number of introductory syllables,

the most common sequence of syllables within a motif, and the most common number of motifs. The eMAH was derived from concatenation of individual MAHs corresponding to each syllable type within its specific context of the canonical song—for example, all spikes corresponding to syllable E in the first motif or all spikes corresponding to syllable E in the second motif (Fig. 1B). Individual MAHs were calculated starting 50 ms before their corresponding syllable.

21. J. J. Gilpin manufactured the devices for chronic

recording. A. S. Dave collected the data for one of the HVC birds. We thank A. S. Dave, S. E. Anderson, and J. A. Kogan, who provided valuable advice and assistance on aspects of the data analysis. M. Konishi and P. S. Ulinski provided useful critiques of the manuscript. Supported by a grant from the Whitehall Foundation (M91-05). A.C.Y. was supported by an NIH predoctoral fellowship (1 F31 MH10151).

26 April 1996; accepted 8 August 1996

Conformational States of the Nuclear Pore Complex Induced by Depletion of Nuclear Ca^{2+} Stores

Carmen Perez-Terzic, Jason Pyle, Marisa Jaconi, Lisa Stehno-Bittel,* David E. Clapham†

The nuclear pore complex (NPC) is essential for the transit of molecules between the cytoplasm and nucleoplasm of a cell and until recently was thought to allow intermediate-sized molecules (relative molecular mass of $\sim 10,000$) to diffuse freely across the nuclear envelope. However, the depletion of calcium from the nuclear envelope of *Xenopus laevis* oocytes was shown to regulate the passage of intermediate-sized molecules. Two distinct conformational states of the NPC were observed by field emission scanning electron microscopy and atomic force microscopy. A central plug occluded the NPC channel after nuclear calcium stores had been depleted and free diffusion of intermediate-sized molecules had been blocked. Thus, the NPC conformation appears to gate molecular movement across the nuclear envelope.

The NPC spans the nuclear envelope and mediates the selective exchange of proteins, mRNA, and ions between the cytoplasm and the nucleus (1). The NPC is a tripartite cylindrical structure surrounded by an octagonal spoked ring complex (2–4). Conformational changes within the NPC and its transporter (which we call the central plug) are thought to regulate movement across the nuclear envelope (3–5). Depletion of the nuclear calcium (Ca^{2+}) stores inhibits diffusion through the NPC of molecules with a relative molecular mass (M_r) of $\sim 10,000$ that lack nuclear localization sequences (6–8). To directly assess whether depletion of Ca^{2+} from nuclear stores triggers a change in the structure of NPC, we used field emission scanning electron microscopy (FESEM) and atomic force microscopy (AFM) to image the NPC central pore. We found that depletion of nuclear cisternal Ca^{2+} , as measured by laser scanning confocal microscopy (7), blocked transport of intermediate-sized molecules and that this block was associated with the appearance of an NPC central plug.

Department of Pharmacology, Mayo Foundation, Rochester, MN 55905, USA.

*Present address: University of Kansas Medical Center, 3901 Rainbow Boulevard, Kansas City, KS 66160–7601, USA.

†To whom correspondence should be addressed. E-mail: clapham@mayo.edu

Nuclear envelopes isolated from *X. laevis* oocytes were imaged by FESEM (9). In nuclei isolated in Ca^{2+} -containing solutions (~ 200 nM), the majority of NPCs displayed typical eightfold symmetry (2–4), but most lacked the central plug (Fig. 1A). The absence of the central plug in NPCs has been attributed to specimen preparation (3, 4, 10, 11). After we first treated nuclei with the physiologically important second messenger, inositol 1,4,5-trisphosphate [$\text{Ins}(1,4,5)\text{P}_3$; $1 \mu\text{M}$ for 10 min] to open Ca^{2+} channels in the nuclear envelope and to deplete Ca^{2+} from nuclear stores (12, 13), we found that the majority of NPCs contained the central plug (Fig. 1B). NPCs from nuclei incubated in Ca^{2+} -containing solution had occupancy of their central pores of $6.9 \pm 0.5\%$ (mean \pm SD; $n = 14$ nuclei, 826 NPCs) compared with $91.9 \pm 1.2\%$ ($n = 10$ nuclei; 630 NPCs) for NPCs of nuclei treated with $\text{Ins}(1,4,5)\text{P}_3$ in the same solution. Treatment of nuclei with other inositol phosphates, which have a low affinity for the InsP_3 receptor and did not release Ca^{2+} from the nuclear store at $1 \mu\text{M}$ concentrations (12, 14), failed to induce the appearance of the central plug in NPCs of isolated nuclear envelopes. In nuclei treated with inositol 1,3,4-trisphosphate [$\text{Ins}(1,3,4)\text{P}_3$; $1 \mu\text{M}$; $n = 8$ nuclei; 488 NPCs] or inositol 1,3,4,5-tetrakisphosphate [$1 \mu\text{M}$ $\text{Ins}(1,3,4,5)\text{P}_4$; $n = 9$ nuclei, 684